

Communication

# 2CALIS doubling the sensitivity of CALIS for calibration of the rf field strength for indirectly observed nuclei

Andrew J. Benie, Ole W. Sørensen \*

*Carlsberg Laboratory, Gamle Carlsberg Vej 10, DK-2500 Valby, Denmark*

Received 4 May 2006

Available online 27 July 2006

## Abstract

A new set of pulse sequences, 2CALIS, that exhibit double sensitivity of the recent CALIS pulse sequences for accurate calibration of the rf field strength for an indirectly observed spin is introduced. The sensitivity gain is a result of not forming heteronuclear coherence transfer gradient echoes although they are excellent for artifact suppression. It is, however, demonstrated that the scheme in 2CALIS for suppression of non  $^{13}\text{C}$ -attached proton magnetization is adequate for calibration of the  $^{13}\text{C}$  rf field strength even on natural abundance samples. A 2CALIS version with Watergate applicable to biomolecules in aqueous solution is also presented and demonstrated both in  $^{13}\text{C}$  natural abundance and on a  $^{13}\text{C}$ ,  $^{15}\text{N}$  enriched protein sample.

© 2006 Elsevier Inc. All rights reserved.

**Keywords:** NMR; Pulse calibration; CALIS; 2CALIS

## 1. Introduction

A recent paper [1] introduced the CALIS-1 and CALIS-2 pulse sequences for accurate calibration of the rf field strength for an indirectly observed spin S via a directly observed spin I. These sequences are attractive because they neither require prior knowledge about the S-spin rf field strength nor exact match of delays to heteronuclear coupling constants and yield clean pure-phase spectra. They include heteronuclear coherence transfer gradient echoes resulting in excellent artifact suppression also for samples with the natural abundance level of isotopes, where e.g.  $^{12}\text{C}$ -attached proton magnetization is eliminated by gradients and optional phase cycles.

In terms of the unitary bounds on spin dynamics [2–4] and apart from relaxation loss during the short pulse sequence, the modulation imposed by the calibration element, and the effect of long-range couplings, the sensitivity of the CALIS sequences are down by 50% com-

pared to a corresponding 1D I-spin spectrum. As in many other experiments, this sensitivity loss comes about by selecting only one out of two coherence transfer pathways by the gradients. While this penalty usually is acceptable in return for excellent artifact suppression, such a high degree of artifact suppression is not always required. Therefore, this paper explores the possibility of modifying the CALIS pulse sequences to the effect of dispensing with formation of heteronuclear coherence transfer gradient echoes and thereby doubling the sensitivity. Hence, the acronym 2CALIS for the new pulse sequences outlined in Fig. 1.

There is an earlier pulse sequence, ROSSANA [5], fulfilling the requirement of being similar to CALIS-2 with double sensitivity, but that sequence requires exact adjustment of several parameters and even then results in relatively large signals from  $^{12}\text{C}$ -attached proton magnetization [5]. The 2CALIS pulse sequences extend ROSSANA and combines it with the CALIS idea of incrementing several S-spin pulses in the calibration [1,6] along with an S-spin filter.

The 2CALIS-2 pulse sequence in Fig. 1a is most easily understood by considering the case of  $\theta = \pi/2$ . The sandwich of the first three I-spin pulses and the first  $2\theta$  S-spin pulse is similar to the INEPT element [7]. After this

\* Corresponding author. Fax +45 3327 4765.

E-mail address: [olews@crc.dk](mailto:olews@crc.dk) (O.W. Sørensen).

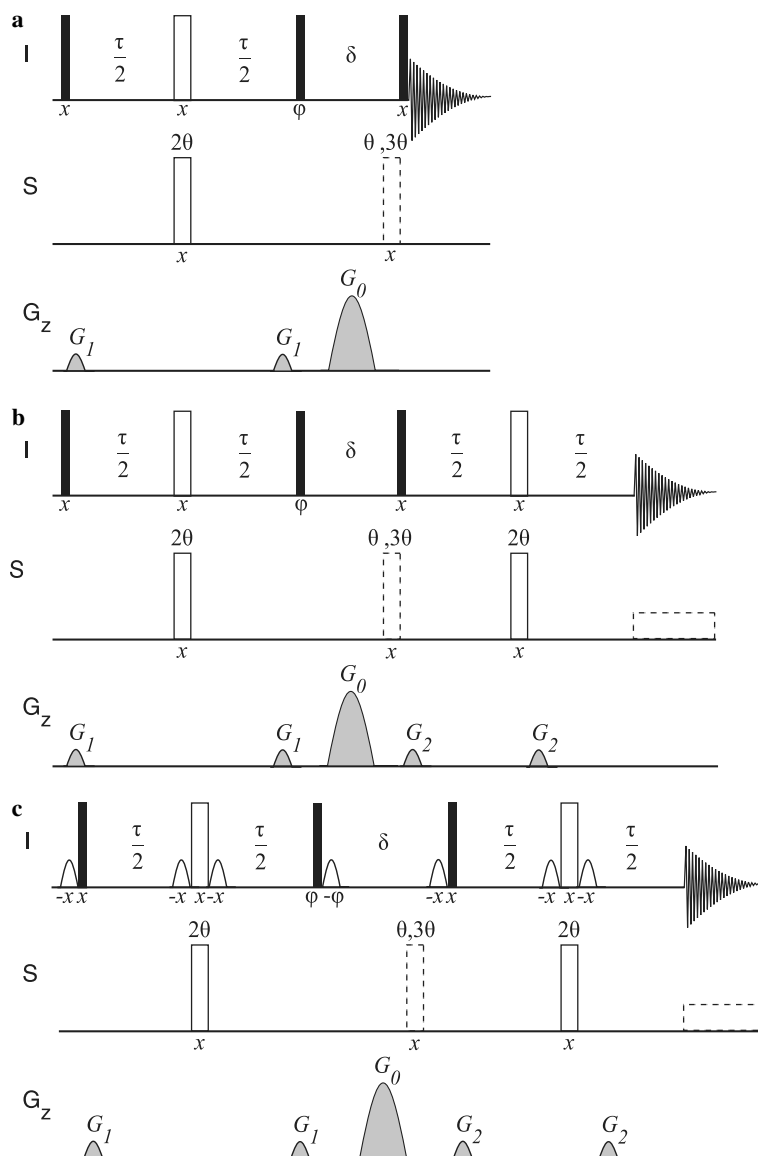


Fig. 1. 2CALIS pulse sequences for calibration of the S-spin (e.g.  $^{13}\text{C}$ ) rf field strength via observation of the I-spin (e.g.  $^1\text{H}$ ) spectrum. On the I-spin channel, filled and open rectangular bars represent non-selective  $\pi/2$  and  $\pi$  pulses, respectively, whilst the shaped pulses correspond to selective  $\pi/2$  pulses applied at the water frequency so as to keep the water magnetization along the  $z$  axis during all delays. A series of spectra with different pulse durations  $\theta$  is run so as to include what is expected to correspond to  $\theta = \pi/2$  where there is a zero-crossing of the signal. The same phasing must be applied to all spectra in the series. The delay  $\tau$  is set to  $(2J)^{-1}$  but is not critical, and  $\delta$  is a gradient delay. The recommended phase and pulse cycles are  $\phi = \{y, y, -y, -y\}$ ,  $\theta/3\theta = \{\theta, 3\theta, 3\theta, \theta\}$  with the receiver phase always alternating between  $x$  and  $-x$ , and the first two steps being the most important. When the  $\theta/3\theta$  element is  $\theta$ , an additional delay corresponding to  $2\theta$  is included to make the pulse sequence have the same length for both steps of the  $\theta/3\theta$  cycle. The gradient  $G_0$  is a purge gradient and the weaker gradients  $G_1$  and  $G_2$  must be set so as not to cause accidental refocusing. (a) Pulse sequence 2CALIS-2 leading to antiphase doublets. (b) Pulse sequence 2CALIS-1 applying S-spin decoupling (shown as a dashed box on the S channel during acquisition) leading to no heteronuclear multiplet structure in the I-spin spectrum. (c) 2CALIS-2 pulse sequence with water flip-back pulses and Watergate [10]; adequate water suppression can in most cases be achieved through the use of the second Watergate element alone. Pulse programs for these 2CALIS pulse sequences can be downloaded from [www.crc.dk/nmr](http://www.crc.dk/nmr).

element, the S-attached I-spin magnetization is longitudinal and in antiphase with respect to the  $J_{\text{IS}}$  coupling constant whilst the I-spin magnetization not coupled to the S-spin is transverse and hence gets purged by the gradient  $G_0$  in the  $\delta$  delay that constitutes a  $z$  filter [8]. The next S-spin pulse is either of flip angle  $\theta$  or  $3\theta$  and key to the calibration, as it for  $\theta = \pi/2$  eliminates the magnetization of interest by transferring it into multiple-quantum coherence,

which is the familiar zero-crossing in this type of experiments [5,6,9]. The  $\theta/3\theta$  two-step cycle combined with alternating receiver phase acts as an S-spin filter, as the non S-spin attached I-spin magnetization is invariant to the flip angle of that pulse. This is in contrast to the S-spin attached I-spin magnetization.

The phase/pulse cycles and gradients in the pulse sequence select the fraction of the S-spin attached I-spin

magnetization that can be said to have experienced a  $\pi$  rotation under the first and a  $0/\pi$  rotation under the second S-spin pulse. These “ideal” pulse settings can also serve to illustrate the inherent relative sensitivities of the 2CALIS and CALIS pulse sequences. In Fig. 2a is shown the spectrum of the anomeric protons in mannose recorded with the 2CALIS-2 pulse sequence with the first and second  $^{13}\text{C}$  pulses set to  $\pi$  and zero, respectively. In Fig. 2b is shown the same but this time including a  $0/\pi$  cycle of the second  $^{13}\text{C}$  pulse, which significantly improves the suppression of non  $^{13}\text{C}$ -attached  $^1\text{H}$  magnetization. Finally, Fig. 2c shows the corresponding spectrum recorded with the CALIS-2 [1] pulse sequence using flip angles  $\pi/2$ ,  $\pi$ , and  $\pi/2$  for the three  $^{13}\text{C}$  pulses in that sequence; the suppression of

non  $^{13}\text{C}$ -attached  $^1\text{H}$  magnetization is the best of the three, but the sensitivity is only half.

It clearly depends on the application and the abundance of the S-spin isotope what degree of suppression of the non S-spin attached I-spin magnetization is required. The 2CALIS-2 version corresponding to the “ideal” in Fig. 2a is the same as the one in Fig. 1a but with only a  $\theta$  pulse at the place of the  $\theta/3\theta$  element and without the cycle of the receiver phase associated with the  $\theta/3\theta$  element. For 2CALIS-2, we usually prefer the full version with the S-spin filter in Fig. 1a corresponding to the “ideal” in Fig. 2b.

The 2CALIS-1 pulse sequence in Fig. 1b extends the 2CALIS-2 pulse sequence in Fig. 1a by a refocusing period to allow S-spin decoupling and thereby about doubling the

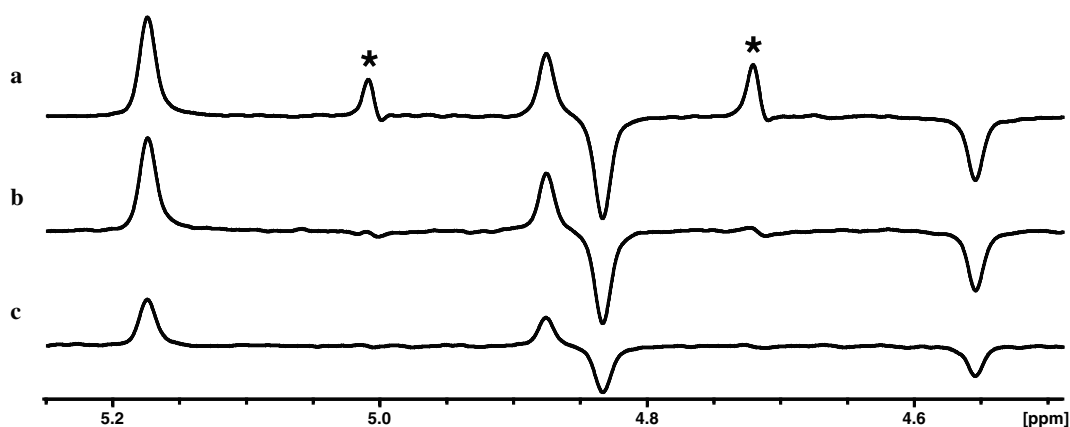


Fig. 2. Excerpts from “ideal” 2CALIS-2 and CALIS-2 spectra with  $^{13}\text{C}$  as the S spin and showing the anomeric protons of mannose recorded on a Varian Unity Inova 500 MHz spectrometer with 8 scans and other parameters identical. (a) Using the 2CALIS-2 pulse sequence in Fig. 1a but with the  $2\theta$  pulse set to  $\pi$ , the  $\theta/3\theta$  element omitted, and with a  $\varphi = \{y, -y\}$  phase cycle combined with the receiver phase alternating between  $x$  and  $-x$ . The  $^{12}\text{C}$ -attached  $^1\text{H}$  signals are marked by asterisks while the interesting signals appear as antiphase doublets. (b) Same as (a) but also including the  $\theta/3\theta$  element set to  $0/\pi$  and with the full phase/pulse cycle indicated in the Fig. 1 caption. (c) Using the CALIS-2 pulse sequence [1] with the three  $^{13}\text{C}$  pulses of that sequence being of flip angles  $\pi/2$ ,  $\pi$ , and  $\pi/2$ , respectively.

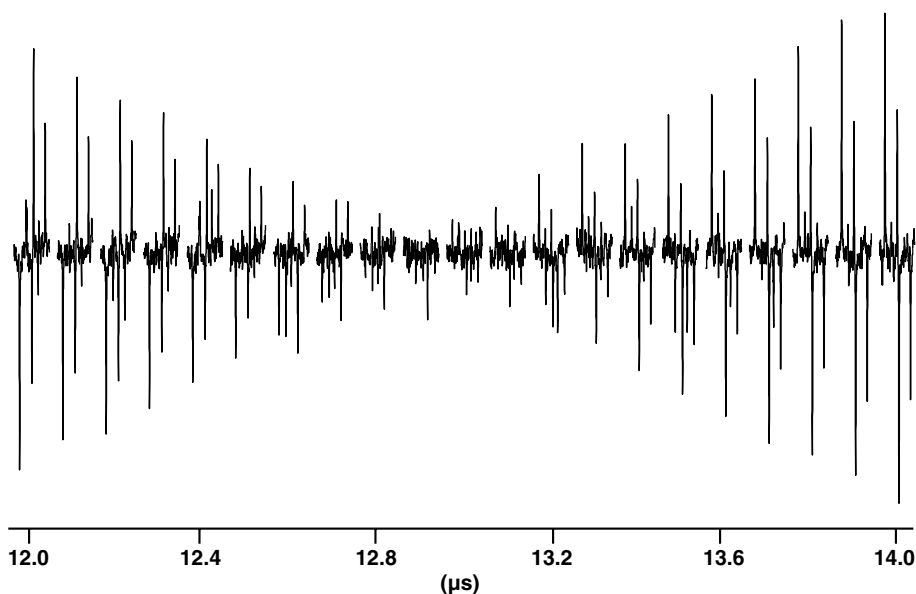


Fig. 3. Natural abundance  $^{13}\text{C}$  2CALIS-2 spectra acquired on 50 mM mannose in  $\text{D}_2\text{O}$  on a Varian INOVA 500 spectrometer, showing the two antiphase doublets corresponding to the  $\alpha$  and  $\beta$  anomeric protons, with varying values for  $\theta$  ( $^{13}\text{C}$ ). The value of  $\tau$  was optimized for the  $\alpha$  anomer ( $^1J_{\text{CH}} = 172$  Hz whereas for the  $\beta$  anomer  $^1J_{\text{CH}} = 158$  Hz) and the number of scans was 8. The zero-crossing was determined to occur at  $t(\pi/2, ^{13}\text{C}) = 12.9$   $\mu\text{s}$ .

sensitivity by collapsing the  $J_{IS}$  doublet into a singlet. Note, however, that for the 2CALIS-1 pulse sequence any residual non S-spin attached I-spin signal will overlap with the signal relevant for the calibration. If such residual signals are so large that they disturb the calibration for  $^{13}\text{C}$  or  $^{15}\text{N}$  natural abundance samples, the choice of S-spin calibration pulse sequence can be between 2CALIS-2 and CALIS-1 exhibiting about the same sensitivity, but with the former and the latter resulting in heteronuclear

doublets and singlets, respectively. In general, calibration using antiphase doublets requires that at least one of the doublet components of a  $^1\text{H}$  multiplet does not overlap with a doublet component of opposite phase from another multiplet. Hence the CALIS-2 and 2CALIS-2 pulse sequences are normally not suitable for protein work.

The 2CALIS-1 pulse sequence in Fig. 1c is adapted for biomolecular applications and aims at maintaining the water magnetization along the  $z$  axis by inclusion of

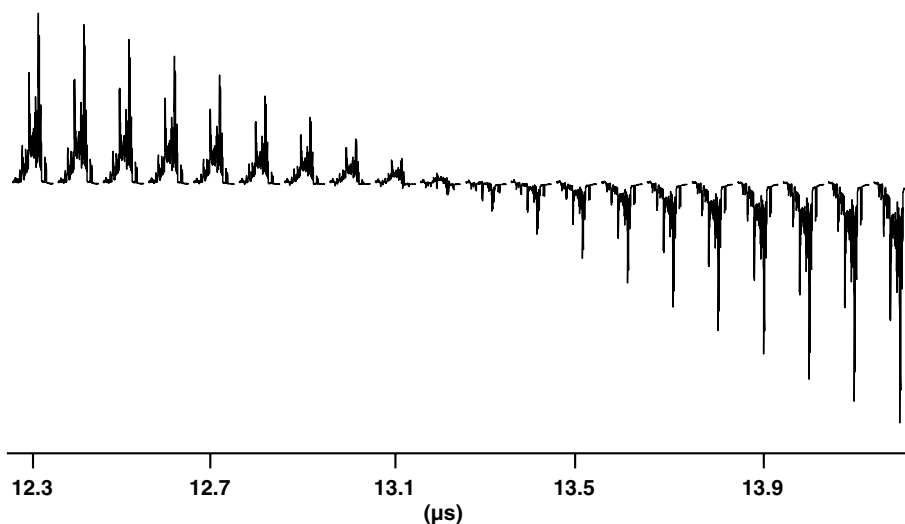


Fig. 4. Excerpts (the  $^1\text{H}$  spectral range from 4.7 to  $-1$  ppm) from  $^{13}\text{C}$  2CALIS-1 spectra acquired on a 0.4 mM  $^{13}\text{C}/^{15}\text{N}$  labeled sample of the protein CI-2 in 90%  $\text{H}_2\text{O}/10\%$   $\text{D}_2\text{O}$  v/v on a Varian Unity Inova 800 MHz spectrometer using the sequence shown in Fig. 1c without the water flip-back pulses and the first Watergate element, i.e. only using the second Watergate element for water suppression. The value of  $\tau$  utilized was set according to  $^1J_{\text{CH}} = 140$  Hz. The carrier frequency for  $^{13}\text{C}$  was placed in the middle of the aliphatic region (40 ppm). The zero-crossing was determined to occur at  $t(\pi/2, ^{13}\text{C}) = 13.25 \pm 0.05 \mu\text{s}$ .

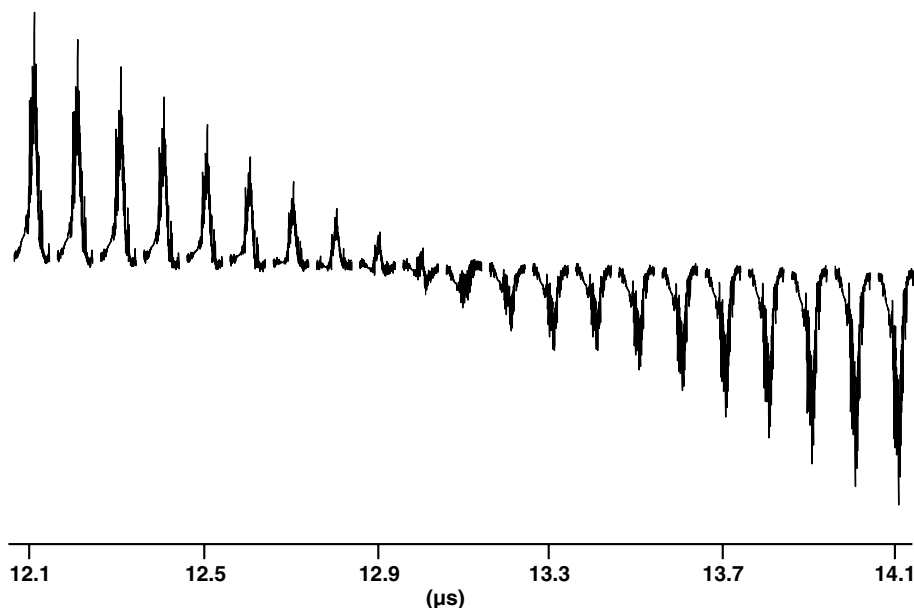


Fig. 5. Excerpts (the  $^1\text{H}$  spectral range from 5 to  $-2$  ppm) from  $^{13}\text{C}$  2CALIS-1 spectra acquired on a 2 mM natural abundance sample of the protein cytochrome c in 100%  $\text{D}_2\text{O}$  on a Varian Unity Inova 800 MHz spectrometer using the sequence shown in Fig. 1b. The value of  $\tau$  utilized was set according to  $^1J_{\text{CH}} = 140$ . The carrier frequency for  $^{13}\text{C}$  was placed in the middle of the aliphatic region (40 ppm). The zero-crossing was determined to occur at  $t(\pi/2, ^{13}\text{C}) = 13.05 \pm 0.05 \mu\text{s}$ .

flip-back pulses and Watergate elements [10]. The corresponding 2CALIS-2 pulse sequence would acquire the FID right after the last  $\pi/2(I)$  pulse.

If, for hardware reasons, the  $3\theta$  pulse around  $\theta = \pi/2$  is short of three times the  $\theta$  pulse by  $\varepsilon$ , a 2CALIS calibration will overestimate the  $\pi/2$  pulse length by  $\varepsilon/4$ . We investigated this potential problem by determining the  $^{13}\text{C}$   $\theta = \pi/2$  and  $3\pi/2$  pulse times directly on mannose in two separate CALIS-2 experiments using the pulse sequence in Ref. [1] with the three  $^{13}\text{C}$  pulses being  $\{\theta, 2\theta, 2\theta\}$  and  $\{\theta, 2\theta, 6\theta\}$ , respectively. On our Varian Unity Inova 500 MHz spectrometer, the result was zero-crossings at 25.8 and 77.4  $\mu\text{s}$  for  $2\theta = \pi$  and  $6\theta = 3\pi$ , respectively, which is the optimum result.

In Fig. 3 is shown a series of excerpts of  $^{13}\text{C}$  2CALIS-2 spectra featuring the anomeric protons of mannose at natural abundance and calibrating the  $^{13}\text{C}$  rf field strength. It can be seen that the suppression of  $^{12}\text{C}$ -attached proton magnetization is sufficiently good as to allow the calibration to be conducted with ease. The incompletely suppressed signals are in the worst case only of the same order of magnitude as the signals used for calibration, and the unsuppressed signals are essentially random in both phase and magnitude.

Fig. 4 shows a 2CALIS-1  $^{13}\text{C}$  calibration performed on the  $^{13}\text{C}/^{15}\text{N}$  labeled protein CI-2 [11] using the sequence in Fig. 1c with only the second Watergate element used for water suppression. Extensive overlap of signals is not a problem for the calibration using this pulse sequence. As suppression of non  $^{13}\text{C}$ -attached magnetization is not an issue for enriched proteins, the 2CALIS-1 pulse sequence—two times as sensitive as the earlier CALIS-1 pulse sequence [1]—is the one of choice for such applications.

Fig. 5 shows an application of the 2CALIS-1 pulse sequence in Fig. 1b to  $^{13}\text{C}$  pulse calibration on cytochrome *c* in natural abundance. The asymmetry in the calibration series around the zero-crossing is due to residual unsuppressed non  $^{13}\text{C}$ -attached magnetization. This, however, does not seriously affect the accuracy of the calibration in this case, as extrapolation from the signal intensities on both sides of the zero-crossing allows a projection of the zero-crossing more or less independent of the residual unsuppressed signals from non  $^{13}\text{C}$ -attached magnetization. If in other applications the residual non  $^{13}\text{C}$ -attached contributions are too severe it is necessary to resort to the earlier CALIS-1 pulse sequence [1] with better artifact suppression at the penalty of a 50% sensitivity reduction.

In conclusion, we have introduced the 2CALIS family of pulse sequences for calibration of the rf field strength for indirectly observed nuclei that has about double sensitivity

of the earlier CALIS family of pulse sequences for the same purpose. This makes 2CALIS-1 the method of choice for most applications, including NMR on enriched proteins and  $^{13}\text{C}$  natural abundance samples. The applications where the inherently less-sensitive CALIS pulse sequences remain the methods of choice include when it is necessary to calibrate via long-range couplings or when the highest degree of suppression of magnetization of the directly observed spins not coupled to the indirectly observed spins is required as e.g. for natural abundance work with some nuclei.

### Acknowledgment

The protein 2CALIS-1 spectra were recorded on the Varian Unity Inova 800 MHz spectrometer of the Danish Instrument Center for NMR Spectroscopy of Biological Macromolecules.

### References

- [1] A.J. Benie, O.W. Sørensen, New methods for calibration of the rf field strength for indirectly observed nuclei, *J. Magn. Reson.* 180 (2006) 317–320.
- [2] O.W. Sørensen, A universal bound on spin dynamics, *J. Magn. Reson.* 86 (1990) 435–440.
- [3] J. Stoustrup, O. Schedletsky, S.J. Glaser, C. Griesinger, N.C. Nielsen, O.W. Sørensen, Generalized bound on quantum dynamics: efficiency of unitary transformations between non-Hermitian states, *Phys. Rev. Lett.* 74 (1995) 2921–2924.
- [4] S.J. Glaser, T. Schulte-Herbrüggen, M. Sieveking, O. Schedletsky, N.C. Nielsen, O.W. Sørensen, C. Griesinger, Unitary control in quantum ensembles. Maximizing sensitivity in coherent spectroscopy, *Science* 280 (1998) 421–424.
- [5] G. Esposito, L. Nadalin, G. Verdonesi, A. Corazza, P. Viglino, M. Fredigo, Improved method for pulse width calibration in indirectly detected experiments, *Magn. Reson. Chem.* 39 (2001) 249–250.
- [6] N.C. Nielsen, H. Bildsøe, H.J. Jakobsen, O.W. Sørensen, Pulse techniques for calibration of the decoupler radiofrequency field strength, *J. Magn. Reson.* 66 (1986) 456–469.
- [7] G.A. Morris, R. Freeman, Enhancement of nuclear magnetic resonance signals by polarization transfer, *J. Am. Chem. Soc.* 101 (1979) 760–762.
- [8] O.W. Sørensen, M. Rance, R.R. Ernst, z filters for purging phase- or multiplet-distorted spectra, *J. Magn. Reson.* 56 (1984) 527–534.
- [9] (a) D.M. Thomas, M.R. Bendall, D.T. Pegg, D.M. Doddrell, J. Field, Two-dimensional  $^{13}\text{C}$ - $^1\text{H}$  polarization transfer J spectroscopy, *J. Magn. Reson.* 42 (1981) 298–306;  
(b) D.M. Doddrell, D.T. Pegg, M.R. Bendall, P. Caha, *Bruker Report* 6 (1980) 18.
- [10] M. Piotto, V. Saudek, V. Sklenár, Gradient-tailored excitation for single-quantum NMR spectroscopy of aqueous solutions, *J. Biomol. NMR* 2 (1992) 661–665.
- [11] A.P. Nanzer, F.M. Poulsen, A.E. Torda, W.F. van Gunsteren, A reassessment of the structure of chymotrypsin inhibitor CI2 using time averaged NMR restraints, *Biochemistry* 33 (1994) 14503–14511.